Centrosomal P4.1-associated protein (CPAP) positively regulates endosome maturation

Radhika Gudi[1], Viswanathan Palanisamy[2], and Chenthamarakshan Vasu[1*]*

[1] Department of Microbiology and Immunology, Medical University of South Carolina, Charleston, SC 29425

[2] Department of Biochemistry, Medical University of South Carolina, Charleston, SC 29425

*Corresponding author (s):

Radhika Gudi

Email: gudi@musc.edu

Or

Chenthamarakshan Vasu
Email: vasu@musc.edu

Running title: Regulation of vesicular trafficking is by CPAP

Key words: Endocytic vesicles, vesicular trafficking, endosome maturation, multi-vesicular body, CPAP.

Abstract

Centrosomal P4.1-associated protein (CPAP) plays a critical role in restricting the centriole length in human cells. Here, we report a novel positive regulatory role for CPAP in endosome maturation during internalized-cell surface receptor trafficking. We found that CPAP is required for targeting ligand-bound cell surface receptor to the lysosome for degradation. While routing of ligand-engaged receptor, which is targeted for degradation or recycling, into early endosomes is not impacted by CPAP-deficiency, sequential transfer of the receptor to late endosome is severely diminished in CPAP-depleted cells. Importantly, activation and recruitment of Rab7, but not Rab5, is compromised upon CPAP depletion indicating its positive regulatory role in early to late endosome transition. Overall, this regulatory role of CPAP in endosome maturation provides new insights in understanding the cellular functions of CPAP, which is well recognized to be critical for centriole duplication and ciliogenesis.

Introduction

Cells can internalize extracellular material, ligands, and surface molecules including receptors by endocytosis. Endocytosis is a fundamental, cellular process that maintains the cellular, tissue and organismal homeostasis. Internalized molecules traffic through, and are sorted by, a series of tubulovesicular compartments including endocytic vesicles(1). Vesicle trafficking pathways play an essential role in the delivery of intra- and extra- cellular cargo, and are critical for cell-to-cell communication(2-6) . Dysregulated cargo delivery pathways can have catastrophic effects and are associated with cancer, neurological diseases, and immunodeficiency(2,7-12).

Post endocytosis, the cell surface receptor cargo is routed through different endosomes, and can have diverse fates such as: 1) be recycled back to the surface, 2) get targeted for degradation, and/or 3) be released outside the cell in exosomes(13) . Early endosomes serve as a sorting nexus for, and play a major role in deciding the cellular fate of, endocytosed cargo(1,14). While majority of the cargo, especially non-ligand-bound receptors, get recycled back to the surface through recycling endosomes(15), regulatory mechanisms exist to ensure that the cargo destined for degradation is routed to lysosomes(16). Lysosome targeting has two additional steps: (i) the formation of an intermediate endocytic organelle referred to as the multi-vesicular body (MVB), also called as multi-vesicular endosome (MVE) or the late endosome(17,18), and (ii) the sequential acquisition and activation of GTPases Rab5 and Rab7(7,19,20). Rab5 to Rab7 conversion is an essential step that marks the maturation of early endosomes to MVBs(21,22). Each MVB possesses a limiting membrane that encloses several smaller vesicles (referred to as intraluminal vesicles; ILVs)(23,24). The direct fusion of mature MVBs with lysosomes that contain lipases, lysozyme and other hydrolytic enzymes facilitates the degradation of cargo, potentially terminating deleterious signal transduction(16,25). MVBs can also be driven towards the plasma membrane to release its content as exosomes(26,27), an essential mode of intra-cellular communication(28-30). Endocytic vesicle transport pathway is known to use microtubules for motor- and Rab- protein regulated movements, and Rab5 to Rab7 acquisition and endosome maturation can occur during the movement along the microtubules(31-37).

Here, we have identified a novel regulatory role for CPAP (centrosomal P4.1 associated protein; expressed by CENPJ gene)/SAS-4, a microtubule/tubulin binding essential centriole biogenesis protein(38) in endosome maturation during endocytic vesicle transport of internalized cell surface

receptor. The centrosome, consists of a pair of centrioles suspended in a peri-centriolar material (PCM) and is the major microtubule organizing centers(MTOC) of mammalian cells(39). Of the several centriolar proteins that can directly interact with microtubules(40-42), CPAP regulates centriolar microtubule growth to produce centrioles of optimum dimension (43). CPAP function is primarily attributed to centriole duplication, specifically restricting the centriole length, and ciliogenesis(38,44-47). Here, employing gain- and loss-of-function methods to assess CPAP function in the ligand-bound epidermal growth factor receptor (EGFR) internalization model, we have determined the positive regulatory role of CPAP in endosome maturation. We found that CPAP is required for efficient trafficking of internalized EGFR to lysosome for degradation. Further, the activation and recruitment of Rab7 to endosome is compromised upon CPAP depletion suggesting its contribution to endosome maturation process, specifically the early to late endosome transition. These novel findings add a new dimension in understanding the cellular functions of CPAP.

Results

CPAP overexpression causes the formation of "MVB-like" structures

The role of CPAP in centriole biogenesis and centrosome function is well established (38,41,48-52). During our studies to determine the interaction between CPAP and other centriolar proteins, we observed that both HEK293T and HeLa cells transfected with GFP-CPAP showed spontaneous formation of punctate structures. These punctate structures were observed not only in most cells that were transiently transfected with GFP-CPAP (**Supplemental Fig. 1A**), but also in cells that were stably transfected with GFP-CPAP under a doxycycline (doxy)-inducible promoter (**Supplemental Fig. 1B**). Immunofluorescence (IF) microscopy of both HEK293T and HeLa cells that transiently express myc-tagged CPAP (myc-CPAP) revealed vesicular structures with distinct membrane localization of anti-myc and anti-CPAP antibody staining **(Supplemental Fig. 2)**, indicating that these are not mere protein aggregates formed due to higher expression levels of GFP- and myc-tagged CPAP and, perhaps, CPAP localizes to the vesicular structures. Although CPAP overexpressing cells that were used in previous report have also shown similar features (42,44,45), the significance of these structures were not further investigated. Importantly, morphologic assessment, by transmission electron microscopy (TEM), of the HEK293T cells transiently transfected with GFP-CPAP and myc-CPAP showed the presence of large, electron

dense bodies containing smaller vesicles **(Fig. 1)**. These electron dense structures have the characteristics of MVB, which are multiple smaller vesicles called intraluminal vesicles (ILVs) bound by a limiting membrane(17,18,25,53). Interestingly, CPAP overexpression associated MVB-like structures were found to be not only higher in number, but also larger in dimensions, than the ones observed in control cells. To determine if CPAP is localized to endocytic vesicles, endosome fractions (Rab5 and Rab7 positive, but β-actin negative) of HEK293T cells that were transiently transfected with control or GFP-CPAP vectors were subjected to IB. As observed in **Fig. 1B**, considerable amounts of GFP-CPAP was detected in this fraction. In addition, immune electron microscopy (IEM) for endogenous CPAP expression in HeLa cells revealed that this protein is present in CD63+ (a marker for MVBs) vesicles/vesicle membrane-like structures **(Fig. 1C & D).** Overall, these results suggest that higher level of CPAP increases the formation of endocytic vesicle-like structures.

CPAP overexpression negatively impacts cellular levels of cell surface receptors

If CPAP overexpression causes constitutive activation of endocytic vesicle transport, then cell surface receptors such as epidermal growth factor receptor (EGFR) could be continuously internalized and degraded in the lysosome when CPAP is overexpressed. To test this notion, first we tested if EGFR can be detected in CPAP overexpression-induced vesicular structures. **Supplemental Fig. 3A** shows that, in both HEK293T and HeLa cells, endogenous EGFR is detectable in several of the CPAP overexpression-induced vesicular structures. Next, we examined the cellular levels of EGFR in doxy-treated HeLa cells that are stably expressing GFP-CPAP under a doxy-inducible promoter. As observed in **Supplemental Fig. 3B,** cellular levels of EGFR, detected by IB, were diminished considerably upon induction of CPAP overexpression, in a dose-dependent manner.

Since CPAP overexpression diminishes EGFR levels, we studied if CPAP depletion impacts the surface and cellular levels as well as the internalization and degradation dynamics of EGFR. First, HeLa cells stably expressing control (scrambled) shRNA and CPAP-shRNA (CPAP-depleted) were examined for cellular **(Fig. 2A)** and surface **(Fig. 2B)** levels of EGFR by IB and FACS. Relative to control shRNA expressing cells, the cellular and surface levels of this receptor were higher in CPAP-depleted cells. Next, these cells were treated with the ligand, EGF for different durations, under cycloheximide (CHX) treatment to block nascent protein synthesis, and the

surface and cellular levels of EGFR were determined. **Fig. 2C** shows that the cell surface levels of EGFR are relatively higher in CPAP-depleted cells compared to control cells at all time-points. However, the surface levels of EGFR in both control and CPAP-depleted cells showed similar degrees of decrease after EGF treatment, as indicated by the fold change in overall mean fluorescence intensity (MFI). This suggests that, although the basal levels of EGFR are different in control and CPAP-depleted cells, the rate of receptor internalization is not significantly altered upon CPAP depletion. IB analysis of EGF treated cells revealed higher cellular levels of EGFR in CPAP depleted cells irrespective of the time-point tested (**Fig. 2D**), suggesting that EGFR degradation pathway is negatively impacted by CPAP depletion. Notably, while majority of the cellular EGFR appears to have degraded in control cells within 120 min post-treatment compared to 0 min time point, CPAP-depleted cells showed the persistence of significant amounts of this receptor at this time-point suggesting its diminished degradation in the absence of CPAP.

To confirm if the effect of diminished EGFR degradation in CPAP-shRNA stably expressing cells is CPAP-depletion specific, similar experiment was conducted using CPAP-siRNA to deplete CPAP and followed by restoration of CPAP expression. HeLa cells were treated with CPAP-specific siRNA to transiently diminish the protein levels, transfected with siRNA-resistant GFP-CPAP cDNA vector(44) to reintroduce CPAP function. These cells were treated with EGF and cellular levels of EGFR were determined by IB. **Fig. 2E** shows that transient depletion of CPAP, similar to its stable depletion (Fig. 2D), also resulted in higher level of cellular EGFR under steady state and upon EGF stimulation, compared to control cells. Similar to cells with stable CPAP depletion using shRNA (Fig. 2D), CPAP siRNA treated cells showed diminished EGF stimulation-induced degradation of this receptor, as indicated by little or no reduction in cellular levels after EGF treatment compared to the 0 min time-point. Importantly, reintroduction of CPAP expression and function appears to restore the ability of ligand treated cells to degrade EGFR as suggested by its diminished cellular levels, post-ligand engagement as compared to 0 h time-point. These observations show defective degradation of internalized cell surface receptors, which are targeted to the lysosome for degradation en route MVB(16), when CPAP levels are low and suggest that CPAP positively contributes to the homeostasis of EGFR-like cell surface receptors.

CPAP depletion results in defective trafficking of cell surface receptor to lysosomes

It is well established that ligand engaged EGFR is degraded in the lysosome(16). Our findings show that CPAP depleted cells showed diminished degradation and higher cellular and surface levels of EGFR. Hence, we examined if ligand engaged EGFR is targeted to the lysosomes for degradation. HeLa cells stably expressing control-shRNA and CPAP-shRNA were treated with Alexa fluor 555-linked EGF on ice, washed and incubated at 37°C for different time-points and stained for the endolysosome/lysosome marker LAMP1, and subjected to confocal IF microscopy. As observed in maximum projection images of **Fig. 3**, control cells showed profound perinuclear clustering of ligand-bound EGFR and colocalization of this receptor with LAMP1, particularly at 60 min post-ligand treatment. However, compared to these control cells, internalized EGFR in CPAP depleted cells showed significantly diminished perinuclear clustering and colocalization with LAMP1. Single Z scan images and quantification of ligand-bound EGFR-LAMP1 co-localized vesicular structures at 60 min time point clearly show inefficient trafficking of EGFR to the lysosomes in CPAP-depleted cells. Of note, lysosome targeting of internalized EGFR appears to be delayed in CPAP depleted cells as indicated by relatively higher perinuclear localization of EGFR in these cells at later time-point (120 min) compared to the 60 min time-point. These observations confirm the defective targeting of internalized receptors to lysosomes under CPAP deficiency.

CPAP depletion results in defective trafficking of cell surface receptor to the MVB/late endosomes

Next, since MVBs fuse with lysosomes to form endolysosomes for delivery of internalized proteins for their degradation(54), localization of ligand engaged EGFR to MVBs was examined. HeLa cells stably expressing control-shRNA and CPAP-shRNA were treated with Alexa fluor 555-linked EGF and stained for MVB/late endosome marker CD63 for different time points and processed in a similar manner as described for the lysosome marker. Similar to LAMP staining, maximum projection images of CD63 staining **(Fig. 4A)** showed profound perinuclear clustering of ligand-bound EGFR and colocalization of this receptor with CD63, particularly at 60 min post-treatment, in control cells. However, in CPAP depleted cells, significantly diminished perinuclear clustering and colocalization of internalized ligand-bound EGFR with CD63 was observed at this time point. Single Z scan images and the quantification of ligand-bound EGFR-CD63 co-localized

vesicular structures at 60 min time point confirms profoundly diminished colocalizaton of CD63 and ligand bound EGFR in CPAP-depleted cells. TEM analysis of EGF treated HeLa cells revealed significantly lower number of electron dense MVB- and endolysosome-like structures in CPAP depleted cells compared to control cells **(Fig. 4B)**. These observations demonstrate defective transport of EGFR to the MVBs when CPAP levels are low.

Targeting of internalized cell surface receptors to the early and recycling endosomes are not affected by CPAP depletion

Internalized ligand activated receptors are routed to the early endosomes, following which they are targeted to the lysosome via MVB for degradation or recycled back to the surface(55). CPAP-depleted cells do not appear to be defective in receptor internalization (Fig. 2) but they show diminished localization of the internalized receptor to the MVB/late endosome and lysosome (Figs. 3 & 4). Hence, we examined whether upstream events of vesicular transport such as early endosome targeting of EGFR, most of which is targeted to lysosome, is affected by CPAP depletion. Control and CPAP depleted HeLa cells that were treated with Alexa flour 555-linked EGF were stained for EEA1 and subjected to confocal IF microscopy. Maximum projection and single Z images, and quantitation of ligand-bound EGFR-EEA1 colocalization showed that EGFR localizes to EEA1 positive vesicular structures at a comparable degree in both control and CPAP depleted cells **(Fig. 5A)**. This suggests that CPAP does not have a regulatory role in sorting of internalized receptors, which are destined for lysosomal degradation, to the early endosomes.

We also examined if the localization of internalized ligand (transferrin; Tfn)-bound transferrin receptor (TfnR), which is primarily recycled back to the cell surface and does not enter the degradation pathway(55), to the early endosome is affected by CPAP depletion. Control and CPAP depleted cells were treated with Tfn for different durations and subjected to confocal microscopy after staining for TfnR and EEA1. **Fig. 5B** shows that, similar to EGFR, TfnR is routed to the early endosome, as indicated by colocalization with EEA1, at comparable degrees in control and CPAP depleted HeLa cells. Further, FACS analysis showed that unlike the EGFR, both control and CPAP depleted HeLa cells maintain comparable levels of surface TfnR under steady state and ligand treatment (**Supplemental Fig. 4**). Overall, in conjunction with the results of Figs. 2-4 showing the cellular levels and subcellular dynamics of EGFR, these observations show that CPAP has a key

regulatory role in the transport of internalized cell surface receptor cargo to the lysosome, late endosome/MVB particularly, but not to the early endosomes.

CPAP depletion does not affect the transport of cell surface receptor to Rab5-positive endosomes

The entry of cell surface receptor cargo into early endosomes activates expression of the GTPase Rab5 on the early endosome membrane (56,57). Further, acquisition of Rab7 expression by Rab5-positive early endosomes, referred to as the Rab5 to Rab7 conversion, triggers signal transduction pathways that are critical for the maturation of early to late endosomes/MVB. This process makes the vesicles competent for fusion with lysosomes(21). Our observations show a positive regulatory role for CPAP in the trafficking of internalized cell surface receptor to late endosome, but it does not affect EGFR localization to the early endosome. Hence, to understand the associated molecular mechanism, first we examined if the ligand-bound EGFR localizes to Rab5 positive endosomes in CPAP depleted cells. As shown in **Fig. 6**, comparable staining pattern and Rab5 positive vesicular structures were observed in both control and CPAP-depleted HeLa cells upon EGF treatment. Further, as seen with maximum projection images of cells at different time-points post-EGF treatment, single Z plane images of 30 and 60 min time-points and quantitation of co-localized vesicles, the degrees of co-localization of ligand-bound EGFR with Rab5 positive vesicular structures were comparable in control and CPAP depleted cells. This suggests that activation and/or recruitment of this GTPase to the endosomes and the localization of ligand-bound receptors to these vesicular structures are not dependent on CPAP.

Rab5 to Rab7 conversion is impaired upon CPAP depletion

Increased abundance of Rab7 positive vesicles after treatment using ligands of cell surface receptors can indicate Rab7 activation (or Rab5-Rab7 conversion) and endosome maturation(58). Since EGFR trafficking to late endosome is diminished upon CPAP depletion, but Rab5 activation is not affected, we determined if CPAP has an impact on the activation of Rab7 and the localization of ligand-bound EGFR to Rab7 positive vesicles. As observed in **Fig. 7A**, a profound increase in the staining intensity and abundance of Rab7 positive vesicular structures were detected in control cells as early as 30 min after treatment with EGF compared to the 0 min time-point. However, CPAP depleted cells showed only a modest increase in Rab7 staining intensity and the abundance of Rab7 positive vesicular structures even at later time-points post-EGF treatment. Importantly, in addition to the lower abundance of Rab7 positive structures, colocalization of ligand-bound EGFR

with Rab7 positive vesicular structures was found to be significantly low in CPAP depleted cells. This is evident from single Z images of cells of 60 and 120 min post-EGF treatment time-points and quantitation showing ligand-bound EGFR-Rab7 colocalization. Overall, these observations suggest that CPAP is critical for the activation and recruitment of Rab7 to facilitate endosome maturation.

Rab5 to Rab7 switch, which can be visualized by determining the degree of their co-localization in vesicular structures, facilitates the early to late endosome transition and endosome maturation (21). Since the abundance of Rab7 vesicles and their colocalization with EGFR positive vesicles was low in CPAP depleted cells and the EGFR localization to MVBs and lysosomes was hampered, we evaluated the colocalization of Rab5 and Rab7, upon EGF ligand binding, in HeLa cells to understand the mechanism of endosome maturation process affected by CPAP. Control and CPAP depleted cells were treated with EGF, stained for Rab5 and Rab7 and imaged using super-resolution Airyscan feature of the Zeiss 880 microscope, which can resolve subcellular distances down to 120nm. **Fig. 7B**, which further validates the observation of Figs. 6 & 7A, shows that Rab7, but not the Rab5 staining intensity is lower in CPAP depleted cells compared to control cells that were stimulated with EGF. Further, single Z images and quantification that shows significantly lower Rab5-Rab7 colocalization suggest that Rab5-Rab7 conversion required for the endocytic transport of cell surface receptors is diminished in CPAP depleted cells. These observations indicate that failure in endosome maturation, specifically the early to late endosome transition, is responsible for the defective trafficking of cell surface receptor cargo to lysosome that is observed upon CPAP depletion.

Discussion

Here, we establish a novel regulatory role for CPAP, an essential centriole biogenesis protein(38), in endosome maturation. CPAP is a microtubule and α-tubulin binding protein and its tubulin-binding function(52,59,60) is important for its function on the centrioles, especially in restricting the centriole length to <500nm(44-46,60). Overexpression of CPAP can cause aberrant long centrioles of up to 3 μm(44-46). In addition, CPAP is required for spindle orientation, which defines normal and asymmetric cell divisions(61). Mutations in the human CENPJ gene has been

associated with microcephaly and Seckel syndrome(62-64). A hypomorphic mouse mutant of the CENPJ gene not only developed microcephaly of the brain but also accumulated centriole duplication defects(65). Recently, it was also shown that CPAP regulates progenitor divisions and neuronal migration in the cerebral cortex. Centrioles can serve as basal bodies, which template the formation of cilia(66). More recently, CPAP has been shown to regulate the length of cilia(44,46,47), perhaps through its centriolar function. Expression of CPAP is cell-cycle regulated (45) and it also determines the timing of cilium disassembly(67). In this study, however, we have uncovered a novel function of this centriole biogenesis protein as a positive regulator of the endocytic vesicle transport of cell surface receptors by promoting endosome maturation.

MVBs serve as critical intermediates towards curbing receptor-mediated signal transduction pathways by sequestering the cargo of early endosome into MVBs and routing these proteins for lysosomal degradation(25). Our results show that CPAP does not regulate the routing of ligand-engaged EGFR into early endosomes. Further, routing for cell surface receptors such as TfnR that are recycled back to the cell membrane from the early endosome also does not appear to be regulated by CPAP. However, our results demonstrate that endosome maturation and transport of the receptor which is destined for lysosome degradation from the late endosome are facilitated by CPAP. This notion has been substantiated by our observation that ligand engaged EGFR colocalization with CD63+ and LAMP+ vesicular structures in cells is profoundly diminished when CPAP is depleted. Perinuclear clustering is the key feature of late endosome/endolysosome entry of protein cargo that is targeted for lysosomal degradation(68). Hence the notion that CPAP facilitates endosome maturation is further supported by our microscopy studies revealing defective perinuclear clustering of EGF+ vesicles in CPAP-depleted cells as compared to control cells. Our ultra-structural studies revealing that higher CPAP expression causes increase in the number and size of MVB-like structures and CPAP depletion results in diminished late endosome/MVB and endolysosome structures suggests that in fact, fewer endocytic vesicles are generated when CPAP expression is low, leading to a blockade in the sequential progression of cargo transport from early to late endosome and the lysosome.

While previous reports were primarily focused on the centriolar localization and function of CPAP, considerable amount of CPAP is also found in the cytoplasmic pool(61). In fact, cytoplasmic-centrosomal shuttling of this protein has been described as a mechanism of regulating centriole

elongation(45,61). Nevertheless, a role of this protein in endosome maturation has never been described. Our studies not only show that overexpressed CPAP is found on the vesicular structures, but also the CPAP protein is detectable on endosomes. However, if the endosome localization of CPAP is required for the vesicular transport function needs to be investigated. In this regard, our observations that CPAP depletion results in the failed recruitment of Rab7 to internalized receptor positive vesicles and defective Rab5-Rab7 conversion provides a key mechanistic explanation for the regulatory role of CPAP in endosome maturation.

Rab7 regulates several steps of the vesicle trafficking processes to release the cargo to be sorted for degradation(69). This serves as a signal for the maturation of early endosomes to late endosomes. Importantly, Rab5 regulates the motility of early endosomes on microtubules (MT) during vesicular transport of the cargo(33). It has been shown that Rab5 dynamically fluctuates on individual early endosomes, linked by vesicle fusion and fission events along with the degradative cargo such as EGFR concentrates in progressively fewer and larger endosomes(57,70). This process occurs when endosomes migrate from the cell periphery to the perinuclear region along the MT where Rab5 is rapidly replaced by Rab7. Since CPAP is a MT-associated protein, with high affinity to bind tubulin, it is possible that this function is compromised when CPAP is absent resulting in a collapse in the endocytic vesicle tethering function, defective cargo movement and vesicle maturation along microtubule filaments, and lack of acquisition of Rab7 by these vesicles. These aspects including interactions of CPAP with various players linked to Rab5-Rab7 conversion and endocytic vesicle movement on MT need to be addressed in future studies. Importantly, motors proteins such as dynein and kinesin that direct cargo transport along the MTs(71) also contribute to centrosome-mediated MT polymerization during cell division(72), (73) suggesting that vesicle transport and centrosome function of CPAP possibly intersect. Studies on the role of these functions together with determining the expression and activation of Rab effectors such as phosphatyidylinositol-3 kinase, MON1A/B-CCZ1 and SNARE proteins such as STX6, STX12, VTI1A, and VAMP4(74,75) will help us dissect the molecular mechanism of CPAP-mediated facilitation of endosome maturation.

In conclusion, our study identifies a novel function for a quintessential centriole biogenesis protein in endosome maturation during the vesicular transport of cell surface receptor cargo targeted for degradation. A wide repertoire of centrosome-associated cellular processes including centriole

duplication, mitotic progression, spindle orientation, and ciliogenesis have been attributed to CPAP. However, whether the newly identified role of CPAP in endosome maturation is required for these processes or is an independent function remains to be studied. Further, whether the centriole-localization of CPAP and its tubulin-binding ability attributes to this newly discovered function on endosome maturation remains to be determined. Nevertheless, novel observations described here will pave the way for new studies to determine if and how the fundamental cellular processes such as centriole duplication and endosome maturation are coupled through CPAP. Importantly, these observations could, potentially, also help better explain the molecular mechanisms of aberrant CPAP expression/function-associated microcephaly, mitotic and spindle positioning errors and ciliopathies

Materials and methods:

Cell lines: HEK293T and HeLa cells were used in this study. These cells were cultured in DMEM media supplemented with 10% FBS, sodium pyruvate, sodium bicarbonate, minimum essential amino acids and antibiotics. Transfection of plasmids was performed using calcium phosphate reagent or TransIT 2020 reagent from Mirus Bio LLC while siRNA was transfected using the TransIT siquest reagent from Mirus Bio LLC.

Plasmids and reagents: GFP-CPAP cDNA expression vector(45) used in this study was kindly provided by Dr. T.K. Tang, University of Taipei, Taiwan. For stable depletion of CPAP, validated lentiviral constructs (pLKO.1) expressing Mission shRNA targeting the following region 5'-CCCACAAGTCTGTGATGATAA-3' in CPAP or scrambled shRNA were purchased from Sigma-Aldrich. For generation of stable cells, lentivirus was generated in 293T cells using accessory plasmids dR8.2 and VSV-G. Target cell line of interest was transduced with virus and selected for shRNA expression by treatment with the drug puromycin (2μg/ml). RNAi resistant construct for expressing GFP-CPAP was kindly provided by Dr. Pierre Gonczy, Swiss Institute for Experimental Cancer Research, Switzerland and the CPAP siRNA targeting sequence has been reported earlier (61).Primary antibodies used in this study: anti-CPAP (Proteintech),-GFP (Santa Cruz Biotech) -actin (Proteintech), -EGFR (Santa Cruz Biotech), TfnR-Alexa fluor 647 (Biolegend) -CD63 (BD Biosciences), -EEA1 (Bethyl labs), -Rab5 (Santa Cruz Biotech), -Rab7 (Proteintech) and -EGFR-PE (Biolegend). Cycloheximide and doxycycline were purchased from

Sigma-Aldrich. Unconjugated EGF ligand was purchased from Tonbo biosciences, Alexa fluor-555 conjugated EGF was from Invitrogen, and holotransferrin ligand was from R&D Biosystems.

Immunofluorescence: Cells grown on coverslips were fixed with 4% paraformaldehyde and permeabilized using 0.1% saponin containing buffer for 30 mins. Blocking with 1% BSA as well as primary and secondary antibody dilutions were made in permeabilization buffer and incubations were done at 37°C. Images were acquired as Z-stacks using either the confocal or superresolution Airyscan unit of Zeiss 880 confocal microscope using the 63X oil immersion objective with n.a. 1.4 as indicated. Optimal setting as suggested by the software was used to acquire the Z sections. Images are presented as maximum intensity projection or a single Z plane as indicated. Image J software was used for image analysis and Adobe photoshop software was used to assemble the images.

Electron microscopy: HEK293T cells transfected with GFP or GFP-CPAP or myc-CPAP constructs for 24h were fixed with 2.5% glutaraldehyde in sodium-Cacodylate buffer (Ted Pella Inc) for 30mins and processed as described in (40,76). After dehydration series with alcohol, cells were embedded in Epoxy resin and cured at 60°C for a couple of days. 70 nm thin sections on copper grids were examined and imaged using the JEOL 1210 transmission electron microscope. For immunogold analysis, HeLa cells treated with EGF ligand for 1h were fixed with 4% PFA and 0.5% glutaradehyde and processed as described (76). 70nm thin sections on nickel grids were stained with anti-CPAP primary and 15nm-gold linked rabbit secondary antibody (EMS Diasum Inc).

EGFR internalization assay: HeLa cells were grown in serum free conditions overnight and incubated with media containing cycloheximide [CHX] (5µg/ml) for 1h. Cells were treated in CHX media with EGF for 1h on ice. Cells were washed with chilled serum free media and transferred to 37°C to induce internalization of receptor. For tracking routing of EGF receptor into vesicles by confocal, Alexa Fluor 555 conjugated EGF (250ng/ml) was used. Untagged EGF (10ng/ml) was used for some experiments. Cell surface EGFR expression was determined by staining cells on ice with anti-EGFR-PE labeled antibody, followed by acquisition using the FACS verse instrument (BD Biosciences). Data was analyzed using the Flowjo software.

Recycling assay: Similar to EGF treatment conditions, HeLa cells were grown in serum free conditions overnight and incubated with media containing CHX (5μg/ml) for 1h. Cells were treated in CHX containing media with holotransferrin ligand for 1h on ice. Cells were washed with serum free media and transferred to 37°C to induce internalization of receptor.

Western blot (WB) and immune blot (IB) assays and endosome isolation: Cells were lysed on ice, lysates were spun at 14000 rpm for 20 min, followed by SDS-PAGE, WB and IB. For determining EGFR degradation, cells were collected at indicated time points and lysed using RIPA lysis buffer containing 0.1% SDS and 1% NP-40 detergent. Total endosome isolation was performed as described before(31).

Image quantification and statistical considerations: Z-stack images were split into single planes and red and yellow pixels were quantified to determine the percentage of colocalization. All experiments were performed at least thrice and data from representative experiments has been shown. *P*-values were calculated using GraphPad Prism statistical analysis software.

Acknowledgements: We would like to thank Dr. T.K. Tang and Dr. Pierre Gonczy for sharing the myc-CPAP/ GFP-CPAP and doxycycline inducible GFP-CPAP expression constructs respectively. We would also like to thank the Cell & Molecular Imaging Shared Resource which is supported by the Hollings Cancer Center, Medical University of South Carolina (P30 CA138313) and the Shared Instrumentation Grant S10 OD018113. We would also like to thank the Flow cytometry and Electron microscopy core facilities at the Medical University of South Carolina. This work was supported by NIH grants R21DE026965 and R21DE026965-02S1 to R.G. and C.V. and MUSC internal funds to C.V.

Data availability: The datasets generated during and/or analyzed during the current study are available from the corresponding author on reasonable request.

References:

1. Scott, C. C., Vacca, F., and Gruenberg, J. (2014) Endosome maturation, transport and functions. *Semin Cell Dev Biol* **31**, 2-10
2. Schmid, S. L., Sorkin, A., and Zerial, M. (2014) Endocytosis: Past, present, and future. *Cold Spring Harb Perspect Biol* **6**, a022509
3. Vieira, A. V., Lamaze, C., and Schmid, S. L. (1996) Control of EGF receptor signaling by clathrin-mediated endocytosis. *Science* **274**, 2086-2089
4. Mettlen, M., Chen, P. H., Srinivasan, S., Danuser, G., and Schmid, S. L. (2018) Regulation of Clathrin-Mediated Endocytosis. *Annual review of biochemistry* **87**, 871-896
5. Neto, H., Collins, L. L., and Gould, G. W. (2011) Vesicle trafficking and membrane remodelling in cytokinesis. *Biochem J* **437**, 13-24
6. Mellman, I., and Nelson, W. J. (2008) Coordinated protein sorting, targeting and distribution in polarized cells. *Nat Rev Mol Cell Biol* **9**, 833-845
7. Stenmark, H. (2009) Rab GTPases as coordinators of vesicle traffic. *Nature reviews. Molecular cell biology* **10**, 513-525
8. Wang, X., Huang, T., Bu, G., and Xu, H. (2014) Dysregulation of protein trafficking in neurodegeneration. *Mol Neurodegener* **9**, 31
9. Griffiths, G. M., Tsun, A., and Stinchcombe, J. C. (2010) The immunological synapse: a focal point for endocytosis and exocytosis. *J Cell Biol* **189**, 399-406
10. Mellman, I., and Yarden, Y. (2013) Endocytosis and cancer. *Cold Spring Harb Perspect Biol* **5**, a016949
11. Mosesson, Y., Mills, G. B., and Yarden, Y. (2008) Derailed endocytosis: an emerging feature of cancer. *Nat Rev Cancer* **8**, 835-850
12. Waterman, H., and Yarden, Y. (2001) Molecular mechanisms underlying endocytosis and sorting of ErbB receptor tyrosine kinases. *FEBS Lett* **490**, 142-152
13. Villasenor, R., Kalaidzidis, Y., and Zerial, M. (2016) Signal processing by the endosomal system. *Curr Opin Cell Biol* **39**, 53-60
14. Tomas, A., Futter, C. E., and Eden, E. R. (2014) EGF receptor trafficking: consequences for signaling and cancer. *Trends Cell Biol* **24**, 26-34
15. Ullrich, O., Reinsch, S., Urbe, S., Zerial, M., and Parton, R. G. (1996) Rab11 regulates recycling through the pericentriolar recycling endosome. *The Journal of cell biology* **135**, 913-924
16. Futter, C. E., Pearse, A., Hewlett, L. J., and Hopkins, C. R. (1996) Multivesicular endosomes containing internalized EGF-EGF receptor complexes mature and then fuse directly with lysosomes. *J Cell Biol* **132**, 1011-1023
17. Piper, R. C., and Katzmann, D. J. (2007) Biogenesis and function of multivesicular bodies. *Annu Rev Cell Dev Biol* **23**, 519-547
18. Gruenberg, J., and Stenmark, H. (2004) The biogenesis of multivesicular endosomes. *Nat Rev Mol Cell Biol* **5**, 317-323
19. Zerial, M. (1993) Regulation of endocytosis by the small GTP-ase rab5. *Cytotechnology* **11 Suppl 1**, S47-49
20. Barbieri, M. A., Roberts, R. L., Gumusboga, A., Highfield, H., Alvarez-Dominguez, C., Wells, A., and Stahl, P. D. (2000) Epidermal growth factor and membrane trafficking. EGF receptor activation of endocytosis requires Rab5a. *The Journal of cell biology* **151**, 539-550
21. Rink, J., Ghigo, E., Kalaidzidis, Y., and Zerial, M. (2005) Rab conversion as a mechanism of progression from early to late endosomes. *Cell* **122**, 735-749
22. Poteryaev, D., Datta, S., Ackema, K., Zerial, M., and Spang, A. (2010) Identification of the switch in early-to-late endosome transition. *Cell* **141**, 497-508

23. White, I. J., Bailey, L. M., Aghakhani, M. R., Moss, S. E., and Futter, C. E. (2006) EGF stimulates annexin 1-dependent inward vesiculation in a multivesicular endosome subpopulation. *EMBO J* **25**, 1-12
24. Futter, C. E., Collinson, L. M., Backer, J. M., and Hopkins, C. R. (2001) Human VPS34 is required for internal vesicle formation within multivesicular endosomes. *The Journal of cell biology* **155**, 1251-1264
25. Woodman, P. G., and Futter, C. E. (2008) Multivesicular bodies: co-ordinated progression to maturity. *Curr Opin Cell Biol* **20**, 408-414
26. Trajkovic, K., Hsu, C., Chiantia, S., Rajendran, L., Wenzel, D., Wieland, F., Schwille, P., Brugger, B., and Simons, M. (2008) Ceramide triggers budding of exosome vesicles into multivesicular endosomes. *Science* **319**, 1244-1247
27. van Niel, G., Porto-Carreiro, I., Simoes, S., and Raposo, G. (2006) Exosomes: a common pathway for a specialized function. *Journal of biochemistry* **140**, 13-21
28. Raposo, G., and Stoorvogel, W. (2013) Extracellular vesicles: exosomes, microvesicles, and friends. *The Journal of cell biology* **200**, 373-383
29. Simons, M., and Raposo, G. (2009) Exosomes--vesicular carriers for intercellular communication. *Current opinion in cell biology* **21**, 575-581
30. Stoorvogel, W., Kleijmeer, M. J., Geuze, H. J., and Raposo, G. (2002) The biogenesis and functions of exosomes. *Traffic* **3**, 321-330
31. Silvis, M. R., Bertrand, C. A., Ameen, N., Golin-Bisello, F., Butterworth, M. B., Frizzell, R. A., and Bradbury, N. A. (2009) Rab11b regulates the apical recycling of the cystic fibrosis transmembrane conductance regulator in polarized intestinal epithelial cells. *Mol Biol Cell* **20**, 2337-2350
32. Bananis, E., Nath, S., Gordon, K., Satir, P., Stockert, R. J., Murray, J. W., and Wolkoff, A. W. (2004) Microtubule-dependent movement of late endocytic vesicles in vitro: requirements for Dynein and Kinesin. *Mol Biol Cell* **15**, 3688-3697
33. Nielsen, E., Severin, F., Backer, J. M., Hyman, A. A., and Zerial, M. (1999) Rab5 regulates motility of early endosomes on microtubules. *Nat Cell Biol* **1**, 376-382
34. Granger, E., McNee, G., Allan, V., and Woodman, P. (2014) The role of the cytoskeleton and molecular motors in endosomal dynamics. *Semin Cell Dev Biol* **31**, 20-29
35. Loubery, S., Wilhelm, C., Hurbain, I., Neveu, S., Louvard, D., and Coudrier, E. (2008) Different microtubule motors move early and late endocytic compartments. *Traffic* **9**, 492-509
36. Vonderheit, A., and Helenius, A. (2005) Rab7 associates with early endosomes to mediate sorting and transport of Semliki forest virus to late endosomes. *PLoS Biol* **3**, e233
37. Huotari, J., and Helenius, A. (2011) Endosome maturation. *EMBO J* **30**, 3481-3500
38. Cho, J. H., Chang, C. J., Chen, C. Y., and Tang, T. K. (2006) Depletion of CPAP by RNAi disrupts centrosome integrity and induces multipolar spindles. *Biochem Biophys Res Commun* **339**, 742-747
39. Sanchez, A. D., and Feldman, J. L. (2017) Microtubule-organizing centers: from the centrosome to non-centrosomal sites. *Curr Opin Cell Biol* **44**, 93-101
40. Gudi, R., Zou, C., Li, J., and Gao, Q. (2011) Centrobin-tubulin interaction is required for centriole elongation and stability. *J Cell Biol* **193**, 711-725
41. Lin, Y. N., Wu, C. T., Lin, Y. C., Hsu, W. B., Tang, C. J., Chang, C. W., and Tang, T. K. (2013) CEP120 interacts with CPAP and positively regulates centriole elongation. *J Cell Biol* **202**, 211-219
42. Hsu, W. B., Hung, L. Y., Tang, C. J., Su, C. L., Chang, Y., and Tang, T. K. (2008) Functional characterization of the microtubule-binding and -destabilizing domains of CPAP and d-SAS-4. *Exp Cell Res* **314**, 2591-2602

43. Sharma, A., Aher, A., Dynes, N. J., Frey, D., Katrukha, E. A., Jaussi, R., Grigoriev, I., Croisier, M., Kammerer, R. A., Akhmanova, A., Gonczy, P., and Steinmetz, M. O. (2016) Centriolar CPAP/SAS-4 Imparts Slow Processive Microtubule Growth. *Dev Cell* **37**, 362-376
44. Kohlmaier, G., Loncarek, J., Meng, X., McEwen, B. F., Mogensen, M. M., Spektor, A., Dynlacht, B. D., Khodjakov, A., and Gonczy, P. (2009) Overly long centrioles and defective cell division upon excess of the SAS-4-related protein CPAP. *Curr Biol* **19**, 1012-1018
45. Tang, C. J., Fu, R. H., Wu, K. S., Hsu, W. B., and Tang, T. K. (2009) CPAP is a cell-cycle regulated protein that controls centriole length. *Nat Cell Biol* **11**, 825-831
46. Schmidt, T. I., Kleylein-Sohn, J., Westendorf, J., Le Clech, M., Lavoie, S. B., Stierhof, Y. D., and Nigg, E. A. (2009) Control of centriole length by CPAP and CP110. *Curr Biol* **19**, 1005-1011
47. Wu, K. S., and Tang, T. K. (2012) CPAP is required for cilia formation in neuronal cells. *Biol Open* **1**, 559-565
48. Gudi, R., Haycraft, C. J., Bell, P. D., Li, Z., and Vasu, C. (2015) Centrobin-mediated regulation of the centrosomal protein 4.1-associated protein (CPAP) level limits centriole length during elongation stage. *J Biol Chem* **290**, 6890-6902
49. Gudi, R., Zou, C., Dhar, J., Gao, Q., and Vasu, C. (2014) Centrobin-centrosomal protein 4.1-associated protein (CPAP) interaction promotes CPAP localization to the centrioles during centriole duplication. *J Biol Chem* **289**, 15166-15178
50. Lin, Y. C., Chang, C. W., Hsu, W. B., Tang, C. J., Lin, Y. N., Chou, E. J., Wu, C. T., and Tang, T. K. (2013) Human microcephaly protein CEP135 binds to hSAS-6 and CPAP, and is required for centriole assembly. *EMBO J* **32**, 1141-1154
51. Tang, C. J., Lin, S. Y., Hsu, W. B., Lin, Y. N., Wu, C. T., Lin, Y. C., Chang, C. W., Wu, K. S., and Tang, T. K. (2011) The human microcephaly protein STIL interacts with CPAP and is required for procentriole formation. *EMBO J* **30**, 4790-4804
52. Hung, L. Y., Tang, C. J., and Tang, T. K. (2000) Protein 4.1 R-135 interacts with a novel centrosomal protein (CPAP) which is associated with the gamma-tubulin complex. *Mol Cell Biol* **20**, 7813-7825
53. Falguieres, T., Luyet, P. P., and Gruenberg, J. (2009) Molecular assemblies and membrane domains in multivesicular endosome dynamics. *Experimental cell research* **315**, 1567-1573
54. Klumperman, J., and Raposo, G. (2014) The complex ultrastructure of the endolysosomal system. *Cold Spring Harb Perspect Biol* **6**, a016857
55. Grant, B. D., and Donaldson, J. G. (2009) Pathways and mechanisms of endocytic recycling. *Nat Rev Mol Cell Biol* **10**, 597-608
56. Bucci, C., Parton, R. G., Mather, I. H., Stunnenberg, H., Simons, K., Hoflack, B., and Zerial, M. (1992) The small GTPase rab5 functions as a regulatory factor in the early endocytic pathway. *Cell* **70**, 715-728
57. Zeigerer, A., Gilleron, J., Bogorad, R. L., Marsico, G., Nonaka, H., Seifert, S., Epstein-Barash, H., Kuchimanchi, S., Peng, C. G., Ruda, V. M., Del Conte-Zerial, P., Hengstler, J. G., Kalaidzidis, Y., Koteliansky, V., and Zerial, M. (2012) Rab5 is necessary for the biogenesis of the endolysosomal system in vivo. *Nature* **485**, 465-470
58. Vanlandingham, P. A., and Ceresa, B. P. (2009) Rab7 regulates late endocytic trafficking downstream of multivesicular body biogenesis and cargo sequestration. *J Biol Chem* **284**, 12110-12124
59. Hung, L. Y., Chen, H. L., Chang, C. W., Li, B. R., and Tang, T. K. (2004) Identification of a novel microtubule-destabilizing motif in CPAP that binds to tubulin heterodimers and inhibits microtubule assembly. *Mol Biol Cell* **15**, 2697-2706
60. Zheng, X., Ramani, A., Soni, K., Gottardo, M., Zheng, S., Ming Gooi, L., Li, W., Feng, S., Mariappan, A., Wason, A., Widlund, P., Pozniakovsky, A., Poser, I., Deng, H., Ou, G., Riparbelli, M., Giuliano,

C., Hyman, A. A., Sattler, M., Gopalakrishnan, J., and Li, H. (2016) Molecular basis for CPAP-tubulin interaction in controlling centriolar and ciliary length. *Nat Commun* **7**, 11874

61. Kitagawa, D., Kohlmaier, G., Keller, D., Strnad, P., Balestra, F. R., Fluckiger, I., and Gonczy, P. (2011) Spindle positioning in human cells relies on proper centriole formation and on the microcephaly proteins CPAP and STIL. *J Cell Sci* **124**, 3884-3893
62. Al-Dosari, M. S., Shaheen, R., Colak, D., and Alkuraya, F. S. (2010) Novel CENPJ mutation causes Seckel syndrome. *Journal of medical genetics* **47**, 411-414
63. Shi, L., Lin, Q., and Su, B. (2014) Human-specific hypomethylation of CENPJ, a key brain size regulator. *Molecular biology and evolution* **31**, 594-604
64. Bond, J., Roberts, E., Springell, K., Lizarraga, S. B., Scott, S., Higgins, J., Hampshire, D. J., Morrison, E. E., Leal, G. F., Silva, E. O., Costa, S. M., Baralle, D., Raponi, M., Karbani, G., Rashid, Y., Jafri, H., Bennett, C., Corry, P., Walsh, C. A., and Woods, C. G. (2005) A centrosomal mechanism involving CDK5RAP2 and CENPJ controls brain size. *Nature genetics* **37**, 353-355
65. McIntyre, R. E., Lakshminarasimhan Chavali, P., Ismail, O., Carragher, D. M., Sanchez-Andrade, G., Forment, J. V., Fu, B., Del Castillo Velasco-Herrera, M., Edwards, A., van der Weyden, L., Yang, F., Sanger Mouse Genetics, P., Ramirez-Solis, R., Estabel, J., Gallagher, F. A., Logan, D. W., Arends, M. J., Tsang, S. H., Mahajan, V. B., Scudamore, C. L., White, J. K., Jackson, S. P., Gergely, F., and Adams, D. J. (2012) Disruption of mouse Cenpj, a regulator of centriole biogenesis, phenocopies Seckel syndrome. *PLoS Genet* **8**, e1003022
66. Breslow, D. K., and Holland, A. J. (2019) Mechanism and Regulation of Centriole and Cilium Biogenesis. *Annu Rev Biochem* **88**, 691-724
67. Gabriel, E., Wason, A., Ramani, A., Gooi, L. M., Keller, P., Pozniakovsky, A., Poser, I., Noack, F., Telugu, N. S., Calegari, F., Saric, T., Hescheler, J., Hyman, A. A., Gottardo, M., Callaini, G., Alkuraya, F. S., and Gopalakrishnan, J. (2016) CPAP promotes timely cilium disassembly to maintain neural progenitor pool. *EMBO J* **35**, 803-819
68. Pu, J., Schindler, C., Jia, R., Jarnik, M., Backlund, P., and Bonifacino, J. S. (2015) BORC, a multisubunit complex that regulates lysosome positioning. *Dev Cell* **33**, 176-188
69. Novick, P., and Zerial, M. (1997) The diversity of Rab proteins in vesicle transport. *Curr Opin Cell Biol* **9**, 496-504
70. Murray, D. H., Jahnel, M., Lauer, J., Avellaneda, M. J., Brouilly, N., Cezanne, A., Morales-Navarrete, H., Perini, E. D., Ferguson, C., Lupas, A. N., Kalaidzidis, Y., Parton, R. G., Grill, S. W., and Zerial, M. (2016) An endosomal tether undergoes an entropic collapse to bring vesicles together. *Nature* **537**, 107-111
71. Driskell, O. J., Mironov, A., Allan, V. J., and Woodman, P. G. (2007) Dynein is required for receptor sorting and the morphogenesis of early endosomes. *Nature cell biology* **9**, 113-120
72. Jones, L. A., Villemant, C., Starborg, T., Salter, A., Goddard, G., Ruane, P., Woodman, P. G., Papalopulu, N., Woolner, S., and Allan, V. J. (2014) Dynein light intermediate chains maintain spindle bipolarity by functioning in centriole cohesion. *The Journal of cell biology* **207**, 499-516
73. Angers, C. G., and Merz, A. J. (2011) New links between vesicle coats and Rab-mediated vesicle targeting. *Seminars in cell & developmental biology* **22**, 18-26
74. Galvez, T., Gilleron, J., Zerial, M., and O'Sullivan, G. A. (2012) SnapShot: Mammalian Rab proteins in endocytic trafficking. *Cell* **151**, 234-234 e232
75. Simons, K., and Zerial, M. (1993) Rab proteins and the road maps for intracellular transport. *Neuron* **11**, 789-799
76. Zou, C., Li, J., Bai, Y., Gunning, W. T., Wazer, D. E., Band, V., and Gao, Q. (2005) Centrobin: a novel daughter centriole-associated protein that is required for centriole duplication. *J Cell Biol* **171**, 437-445

Methods

Fig. 1: CPAP overexpression causes the formation of MVB-like structures. A. HEK293T cells were transfected with control vector, or GFP-CPAP or myc-CPAP expression vectors for 24h as described for Supplemental Fig. 1, fixed with paraformaldehyde and processed for TEM, and representative images are shown in upper panels. Numbers of MVB-like structures per unit cell [GFP n=13; GFP-CPAP n=43] and diameters of individual MVB like structures [GFP n=24; GFP-CPAP n=161] were calculated from three separate experiments for control and GFP-CPAP vector transfected cells and the Mean ± SD values (lower panels) are shown. *p*-value by chi^2 test comparing the ratios of MVBs with <1000nm and >1000nm sizes or ratios of cells/images with <5 and >5 MVBs between control and GFP-CPAP cells. Note: MVB number and size were determined in transfected cell preparations containing cells with and without GFP expression in an unbiased manner for both groups. **B.** Endosome rich fractions were prepared from HEK293T cells transfected with GFP or GFP-CPAP for 24h and subjected to IB to detect GFP-CPAP, Rab5, Rab7, and β-actin. **C.** HeLa cells were subjected to serum starvation overnight, treated with cycloheximide and EGF ligand on ice, washed and incubated for 1h at 37ºC, and processed for IEM after staining 70-nm thin sections on nickel grids with anti-CPAP antibody followed by anti-rabbit-gold (15nm) linked secondary antibody and imaged using JEOL 1210 TEM. Yellow arrows show examples of CPAP localization to vesicular structures. **D**. Sections were also stained with anti-CPAP and anti-CD63 primary antibodies followed by anti-rabbit-gold (15nm) and anti-mouse gold (6 nm) linked secondary antibodies. Yellow arrows indicate CPAP and white arrows indicate CD63 localization to vesicular structures.

Fig. 2: CPAP depletion increases surface and cellular levels of EGFR. HeLa cells stably expressing control-shRNA or CPAP-shRNA were examined for CPAP depletion and EGFR levels by WB (**A**) and surface EGFR levels by FACS **(B)**. These cells were subjected to serum starvation overnight, treated with cycloheximide for 1h and EGF, washed and incubated for indicated durations, and subjected to FACS analysis to detect surface levels of EGFR after staining using anti-EGFR antibody. Representative overlay graphs for each time-point **(C, upper panel)**, mean MFI values of three independent assays (**C, lower left panel**) and EGF treatment induced fold changes in EGFR specific MFI values, relative to 0 min time-point, (**C, lower right panel**) are

shown. **D.** Cells stimulated using EGF as described in panel C were also subjected to WB to detect EGFR and β-actin. **E.** HeLa cells treated with control-siRNA or CPAP-siRNA, along with CPAP-siRNA treated cells that express siRNA-resistant GFP-CPAP under doxy-inducible promoter, were treated with EGF as described for panel D and subjected to WB analysis to detect GFP-CPAP, EGFR and β-actin. GFP-CPAP expressing cells were treated with doxy for 24h before initiating this assay.

Fig. 3: CPAP depletion results in defective targeting of internalized cell surface receptor to the lysosome. HeLa cells expressing control-shRNA or CPAP-shRNA were incubated with Alexa fluor 555-conjugated EGF ligand and left on ice for 1h. Cells were washed with serum free media and transferred to 37°C to initiate receptor internalization. Cells were fixed at indicated time-points, permeabilized and stained for LAMP1 to mark lysosomes. Images were acquired as Z-stacks using Zeiss 880 and representative maximum projection images (upper panel) and single Z plane of relevant images of 60 min time-point (lower left panel) are shown. Mean ± SD values of percentage EGF+ vesicular structures that co-localize with LAMP1 staining from three independent experiments (at least 20 cells/experiment) are also shown (lower right panel).

Fig. 4: CPAP depletion results in defective trafficking of internalized cell surface receptor to MVB/late endosome. A. HeLa cells expressing control-shRNA or CPAP-shRNA were incubated with Alexa fluor 555-conjugated EGF ligand and left on ice for 1h. Cells were washed with serum free media and transferred to 37°C to initiate receptor internalization. Cells were fixed at indicated time-points, permeabilized and stained for CD63 to mark MVB/late endosome. Images were acquired as Z-stacks using Zeiss 880 and representative maximum projection images (upper panel) and single Z plane of relevant images of 60 min time-point (lower left panel) are shown. Mean ± SD values of percentage EGF+ vesicular structures that co-localize with CD63 staining from three independent experiments (at least 20 cells/experiment) are also shown (lower right panel). **B.** HeLa cells expressing control-shRNA or CPAP-shRNA were treated with EGF for 1 h and subjected to TEM analysis, and representative images (left panel) and mean ± SD values (right panel) of number of late endosome [MVBs (M) and endo-/lysosomes (electron dense bodies; EL and L) are shown. Vesicles were quantified for at least 15 cells/group.

Fig. 5. CPAP depletion has no impact on trafficking of cell surface receptor to early endosomes. **A.** HeLa cells expressing control-shRNA or CPAP-shRNA were incubated with Alexa fluor 555-conjugated EGF ligand and left on ice for 1h. Cells were washed with serum free media and transferred to 37°C to initiate receptor internalization. Cells were fixed at indicated time-points, permeabilized and stained for EEA1 to mark early endosomes. Images were acquired as Z-stacks using Zeiss 880 and representative maximum projection images (upper panel) and single Z plane of relevant images of 30 min time-point (lower left panel) are shown. Mean ± SD values of percentage EGF+ vesicular structures that co-localize with EEA1 (lower right panel) staining from three independent experiments (at least 15 cells/experiment) are also shown. **B.** HeLa cells expressing control-shRNA or CPAP-shRNA were incubated with holotransferrrin and processed similarly to that for panel A and stained for TfR and EEA1. Maximum projection images Left panel) and single Z plane of relevant images of 30 min time-point (upper right panel) are shown. Mean ± SD values of percentage TfR+ vesicular structures that co-localize with EEA1 (lower right panel) staining from three independent experiments (at least 15 cells/experiment) are also shown.

Fig. 6. CPAP depletion does not affect trafficking of cell surface receptor to Rab5-positive endosomes. HeLa cells expressing control-shRNA or CPAP-shRNA were incubated with Alexa fluor 555-conjugated EGF ligand and left on ice for 1h. Cells were washed with serum free media and transferred to 37°C to initiate receptor internalization. Cells were fixed at indicated time-points, permeabilized and stained for Rab5. Images were acquired as Z-stacks using Zeiss 880 and representative maximum projection images (upper panel) and single Z plane of relevant images of 30 and 60 min time-points (lower left panel) are shown. Mean ± SD values of percentage EGF+ vesicular structures that co-localize with Rab5 (lower right panel) staining from three independent experiments (at least 20 cells/experiment) are also shown.

Fig. 7. CPAP depletion results in aberrant trafficking of internalized cell surface receptor to Rab7-positive endosomes. A) HeLa cells expressing control-shRNA or CPAP-shRNA were incubated with Alexa fluor 555-conjugated EGF ligand and left on ice for 1h. Cells were washed with serum free media and transferred to 37°C to initiate receptor internalization. Cells were fixed at indicated time-points, permeabilized and stained for Rab7. Images were acquired as Z-stacks

using Zeiss 880 confocal and representative maximum projection images (upper panel) and single Z plane of relevant images of 60 and 120 min time-points (lower left panel) are shown. Mean ± SD values of percentage EGF+ vesicular structures that co-localize with Rab7 (lower right panel) staining from three independent experiments (at least 20 cells/experiment) are also shown. **B)** HeLa cells expressing control-shRNA or CPAP-shRNA were incubated with unconjugated EGF for 60 min, co-stained for Rab5 and Rab7 and the images were acquired using the Airyscan unit of Zeiss 880 microscope. Representative maximum projection images (left panel) and single Z plane of relevant images of 60 min time-point (middle panel) are shown. Mean ± SD values of percentage Rab7+ vesicular structures that co-localize with Rab5 (right panel) staining from three independent experiments (at least 15 cells/experiment) are also shown.

Fig. 1

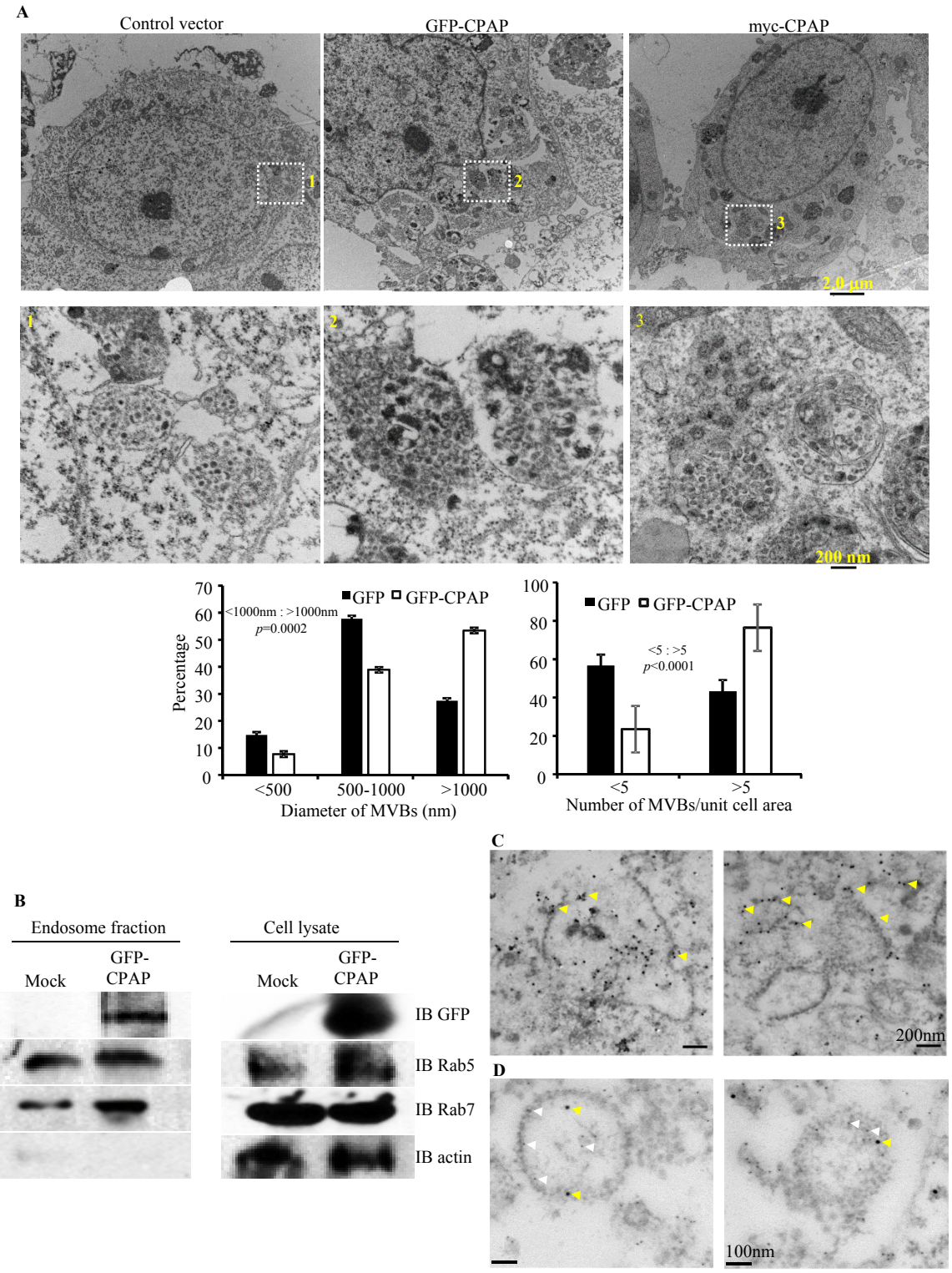

Fig. 2

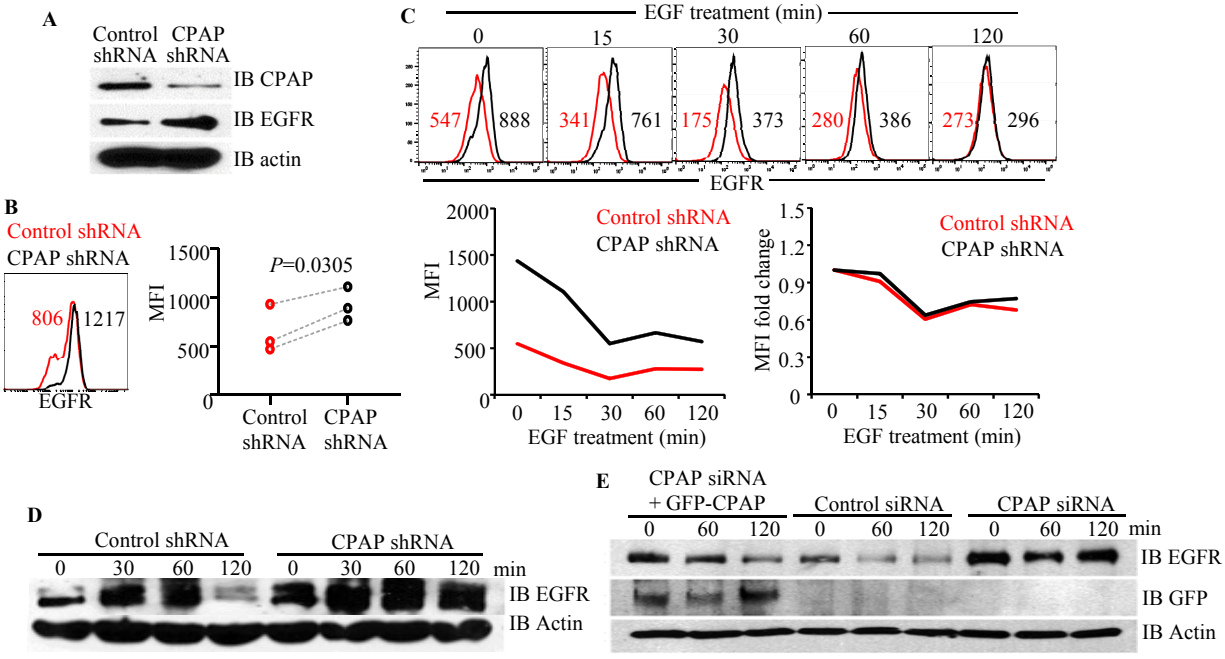

Fig. 3

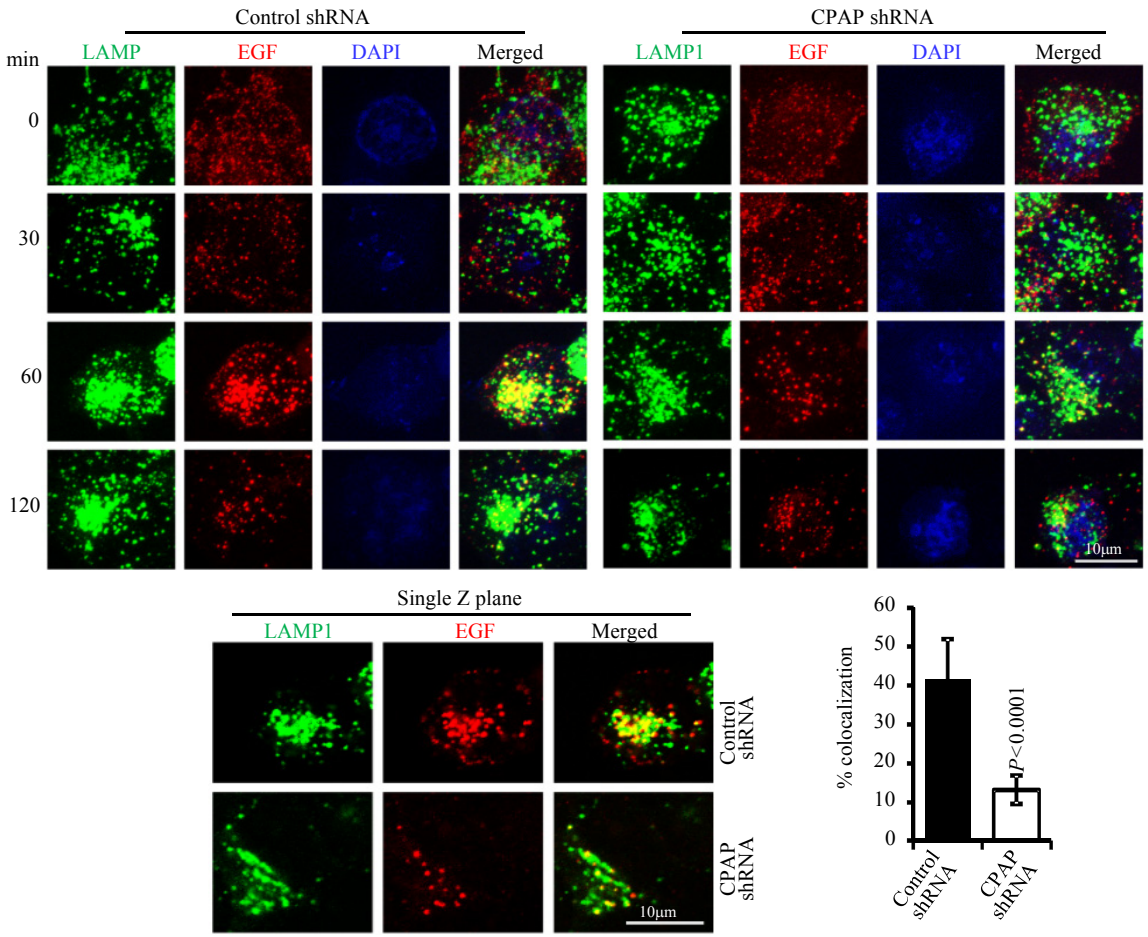

Fig. 4

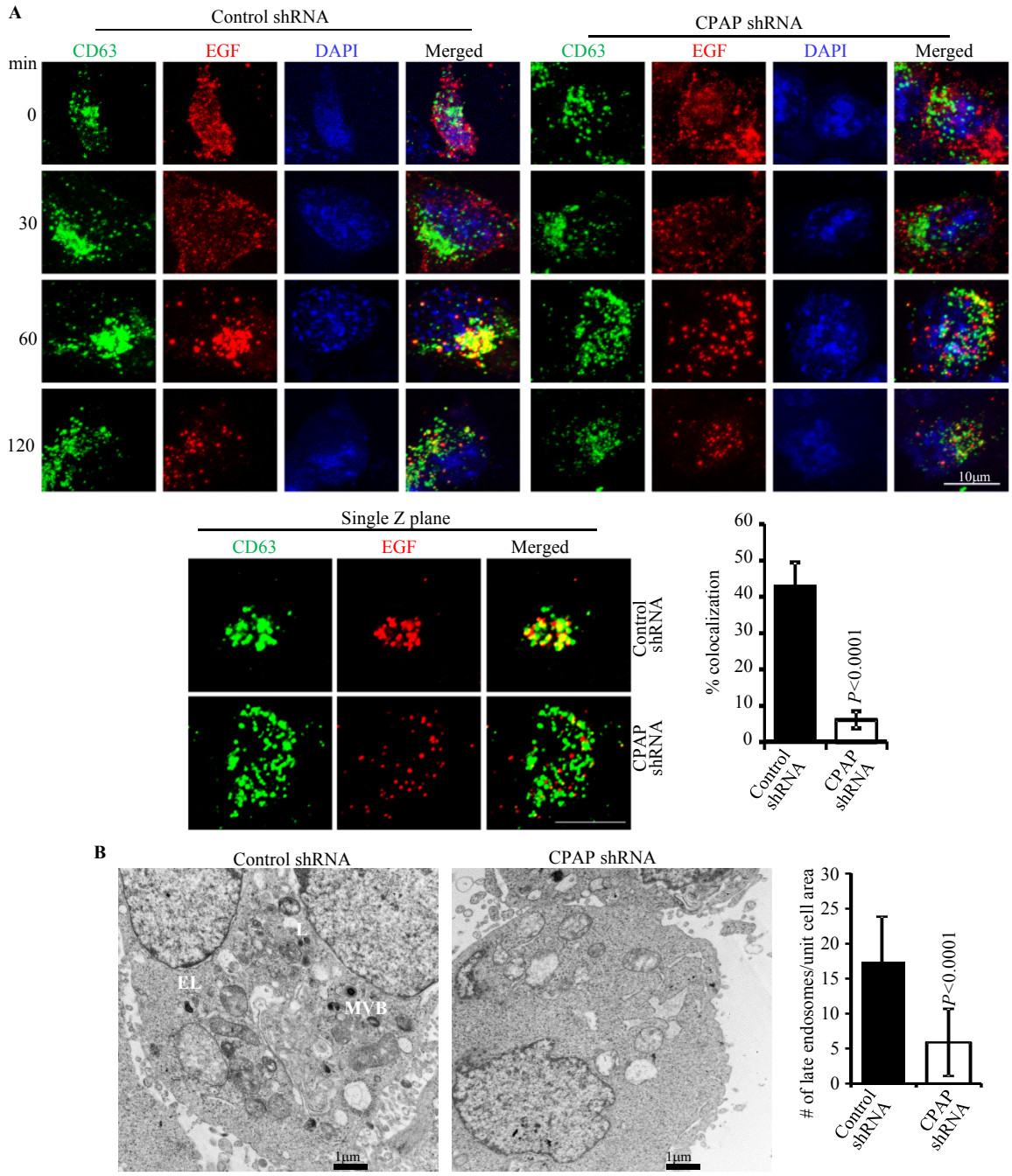

Fig. 5

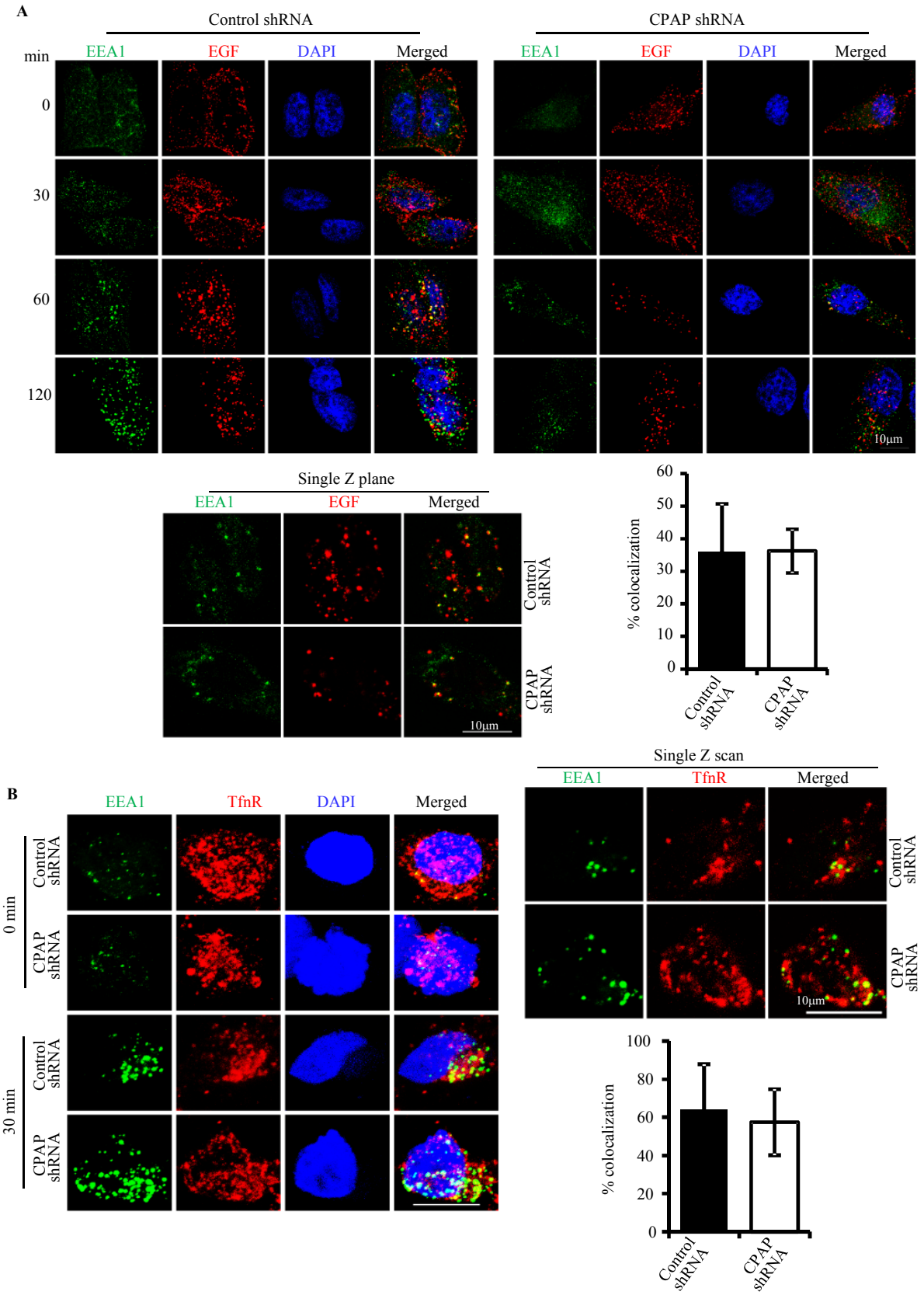

Fig. 6

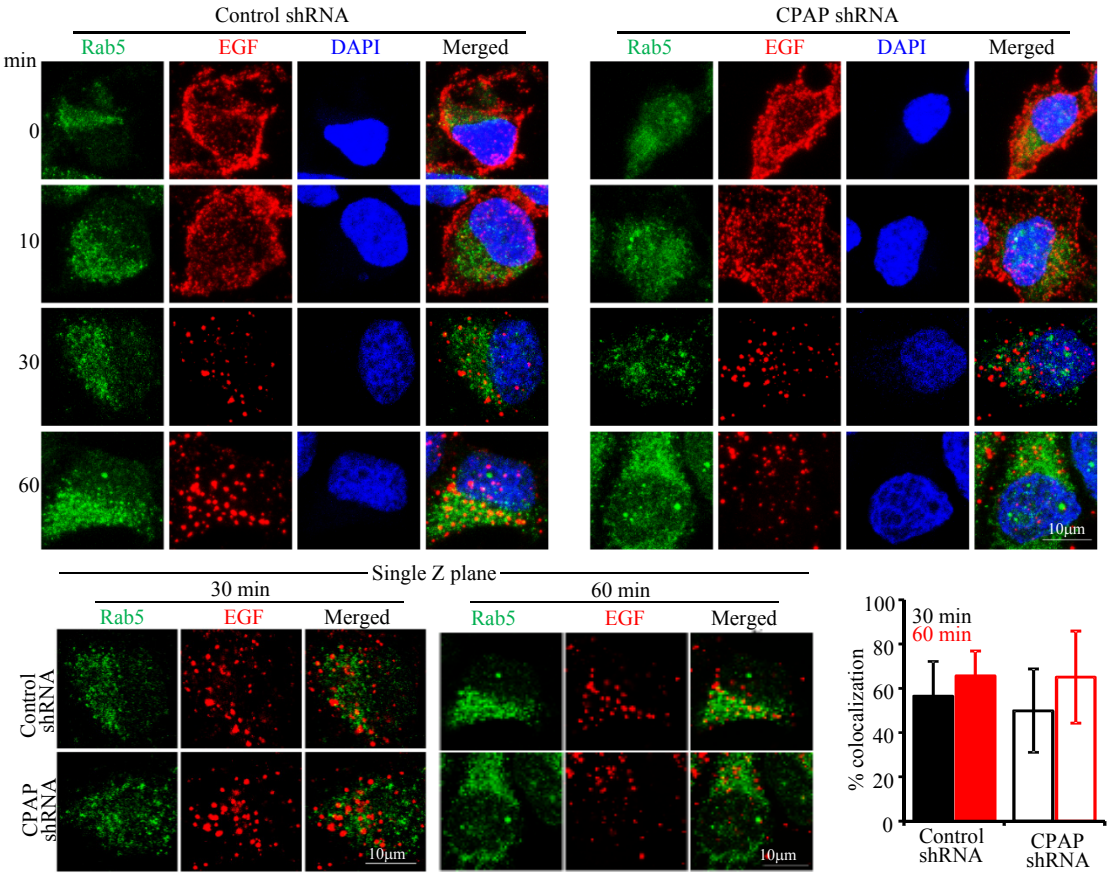

Fig. 7